



HAL
open science

Heliospheric conditions that affect the interstellar gas inside the heliosphere

D. R. McMullin, M. Bzowski, E. Möbius, A. Pauluhn, R. Skoug, W.
Thompson, M. Witte, R. von Steiger, D. Rucinski, D. Judge, et al.

► **To cite this version:**

D. R. McMullin, M. Bzowski, E. Möbius, A. Pauluhn, R. Skoug, et al.. Heliospheric conditions that affect the interstellar gas inside the heliosphere. *Astronomy and Astrophysics - A&A*, 2004, 426 (3), pp.885-895. 10.1051/0004-6361:20047147 . insu-03590965

HAL Id: insu-03590965

<https://insu.hal.science/insu-03590965>

Submitted on 28 Feb 2022

HAL is a multi-disciplinary open access archive for the deposit and dissemination of scientific research documents, whether they are published or not. The documents may come from teaching and research institutions in France or abroad, or from public or private research centers.

L'archive ouverte pluridisciplinaire **HAL**, est destinée au dépôt et à la diffusion de documents scientifiques de niveau recherche, publiés ou non, émanant des établissements d'enseignement et de recherche français ou étrangers, des laboratoires publics ou privés.

Coordinated observation of local interstellar helium in the Heliosphere
**Heliospheric conditions that affect the interstellar
gas inside the heliosphere**

D. R. McMullin¹, M. Bzowski², E. Möbius³, A. Pauluhn⁴, R. Skoug⁵, W. T. Thompson⁶, M. Witte⁷,
R. von Steiger⁴, D. Rucinski², D. Judge⁸, M. Banaszekiewicz², and R. Lallement⁹

¹ Space Sciences Center, University of Southern California, Los Angeles, CA 90089, USA
Praxis, Inc., Alexandria, VA, USA
e-mail: mcmullind@pxi.com

² Space Research Centre PAS, Bratytcka 18A, 00-716 Warsaw, Poland

³ Space Science Center and Department of Physics, University of New Hampshire, Durham, NH 03824, USA

⁴ International Space Science Institute, 3012 Bern, Switzerland

⁵ Los Alamos National Laboratory, Los Alamos, NM 87545, USA

⁶ Goddard Space Flight Center, Greenbelt, MD 20771, USA

⁷ Max-Planck-Institut für Aeronomie, 37191 Katlenburg-Lindau, Germany

⁸ Space Sciences Center, University of Southern California, Los Angeles, CA 90089, USA

⁹ Service d'Aéronomie du CNRS, BP 3, 91371, Verrières-le-Buisson, France

Received 26 January 2004 / Accepted 23 June 2004

Abstract. The interstellar gas that flows through the heliosphere is strongly affected by ionization close to the Sun, in particular solar photoionization, electron impact, and charge exchange. Therefore, the interpretation of any observation of interstellar gas in the inner heliosphere hinges upon the accurate knowledge of these effects and their variations. In addition, the irradiance and line profile of the relevant solar spectral line are needed to properly interpret resonant backscattering observations of the interstellar neutral gas. With instrumentation on ACE, SOHO and Wind, continuous monitoring of these important environmental conditions simultaneously with a multitude of interstellar gas observations has become possible for the first time. In this paper we present a compilation of the processes and parameters that affect the distribution of interstellar helium inside the heliosphere and their observation, including the irradiance and line profile of the He 58.4 nm line. We also make the connection to proxies for these parameters and evaluate their accuracy in order to expand the time period of coverage wherever possible.

Key words. ISM: general – ISM: atoms – interplanetary medium – plasmas

1. Introduction

As the heliosphere travels through the local interstellar cloud (LIC), the neutral particles enter on essentially straight lines, whereas the ionized particles are deflected by the interplanetary magnetic field. Approaching the Sun, however, the interstellar neutrals are bent on hyperbolic (Keplerian) orbits and, at the same time, exposed to ionizing forces that decrease the neutral population. For observations from within the heliosphere, information about the LIC is contingent upon these effects. LIC parameters are generally deduced from the spatial and velocity distribution of the interstellar gas in the inner heliosphere. Therefore, in order to properly deduce the parameters of the LIC, as observed from within the inner heliosphere, the natural conditions that affect the interstellar gas inside the heliosphere must be accounted for.

After hydrogen, helium is the most abundant element in the universe. Because of its high ionization potential, He is the species that comes closest to the Sun as neutral gas. Finally, it is not affected by the interface between the LIC and the

heliosphere (Fahr & Ripken 1984; Izmodenov et al. 1999; Müller et al. 2000) and thus reflects most closely the conditions in the LIC. Currently, helium is the only interstellar gas species that can be observed with all three diagnostic techniques in the inner heliosphere, i.e., by using backscattering of solar UV radiation (Weller & Meier 1981; Dalaudier et al. 1984; Chassefière et al. 1986; Flynn et al. 1998), by observing pickup ions (Möbius et al. 1985, 1995; Gloeckler et al. 1997), and by imaging directly the neutral gas flow through the solar system (Witte et al. 1996).

When interstellar neutral helium particles approach the heliosphere they pass through the heliopause essentially unimpeded. On approaching the Sun on Keplerian orbits they are increasingly subject to ionization. Therefore, when observing interstellar neutrals at a specific point in the heliosphere, their density has been reduced due to ionization losses.

The only space instrument to date that has measured interstellar neutral particles is the GAS sensor on Ulysses (Witte et al. 1992) which has now accumulated observations of

interstellar helium over almost a complete solar cycle (Witte et al. 2003). At each point in space the particles reach the spacecraft from two directions, either directly (i.e., on the inward branch of the hyperbolic orbit) or indirectly (on the outward branch). These arrival directions, together with the orbit and attitude data of the spacecraft, allow reconstruction of the density, velocity, and temperature of the particles “at infinity” (Banaszkiewicz et al. 1996). However, the determination of the density depends directly on the rate with which neutral particles were lost along the way due to ionization processes.

Pickup ions, i.e., ions that have been picked up by the solar wind following ionization, provide valuable insight into the state of the local interstellar medium (Möbius et al. 1985; Gloeckler et al. 1997). Most of the pickup ion constituents are interstellar neutrals that flow into our solar system. They become ionized through photoionization, electron impact, and charge exchange, and are then picked up and carried by the solar wind to the outer limits of the solar system. These pickup ions are then accelerated at the solar wind termination shock, producing anomalous cosmic rays (Fisk et al. 1974). Therefore, knowledge about pickup ions not only provides data about the local interstellar medium (LISM), but also gives a direct account of an important source population for further acceleration. In the case of pickup ions, knowledge of the ionization rates of inflowing interstellar atoms is also necessary to determine the neutral source distribution from the pickup ion observations (Möbius et al. 1985, 1988, 1995, 1999; Rucinski & Fahr 1989; Gloeckler et al. 1993; Geiss et al. 1994). It should be noted here that the ionization rates influence the analysis of pickup ion measurements in two ways. Firstly, the observed pickup ion flux is the product of the local neutral gas density and the ionization rate for the past few days, over which the pickup ion spectrum has been accumulated according to their transport with the solar wind. Secondly, as for the other measurements in the inner heliosphere, the integral effect of the ionization during the flow of the interstellar neutrals into the inner heliosphere determines by how much the local density is depleted over the original density in the LIC. The ionization rates for each individual species are needed to derive the absolute density as well as the elemental composition ratios in the nearby interstellar medium. Only isotopic ratios can be derived directly from observed ratios, because the ionization rates are almost identical for isotopes of the same element.

A third diagnostic technique used in observing interstellar helium is UV backscattering. As interstellar neutral helium flows through the heliosphere, the solar He-Lyman- α (58.4 nm) line resonantly scatters back from the particle and can be detected using appropriate instrumentation. As in the two previously described observing techniques (neutral particles and pickup ions), the UV backscattering technique is also sensitive to the ionization loss rates, the absolute solar 58.4 nm irradiance, and the profile of the solar 58.4 nm line.

In the past, the interpretation of all these observations has suffered from inadequate modeling and problems related to the lack of appropriate simultaneous observations of the relevant parameters. Increasingly sophisticated experimental insight into the processes that shape the distribution of interstellar helium inside the heliosphere, obtained during recent years,

has made it clear that coordinated measurements of these parameters could significantly improve the convergence of results of interstellar helium studies performed with the use of different, independent experimental methods.

Over the past years a coordinated set of observations has been compiled that has been analyzed in a collaborative effort. The results of this analysis are presented in separate papers on neutral gas observations by Witte (2004), on pickup ion measurements by Gloeckler et al. (2004), and on UV backscattering observations by Lallement et al. (2004c). A synopsis of the combined effort is given by Möbius et al. (2004). In this paper we will focus on the ancillary data needed to appropriately interpret the observations of interstellar helium. This includes information on all processes that contribute to the ionization of interstellar helium and on the relevant solar UV line for the backscattering observations.

In particular, we will review the time series of the solar EUV flux, which is the dominant source for ionization of interstellar helium, measured with the SOHO Solar EUV Monitor (SEM) instrument. In addition, we will show that this ionizing EUV flux tracks very well with an often used proxy, i.e., the Mg II index. This finding will allow us to extend the improved knowledge of the ionization rates to earlier times. We will also review available electron ionization data from the Ulysses and Advanced Composition Explorer (ACE) spacecraft and extrapolate them towards the Sun using the earlier Helios measurements. We will also use information on solar wind speed, density, and α -particle abundance at various heliolatitudes and over a range of solar activity levels to evaluate the effects due to charge exchange ionization.

Finally, important information required to interpret observations of the helium backscatter glow is contained in the solar He 58.4 nm line profile and its disk-integrated intensity variations. In the absence of a sufficiently long time series of observations, these parameters must partially be estimated using index proxies.

2. Ionization

For the observation techniques available in the inner heliosphere for analysis of the LIC, ionization processes are extremely important to interpret the measurements and their quality is directly dependent on the accurate knowledge and understanding of these effects and their variations. Three sources of ionization that contribute to the loss rate of neutral helium are solar photoionization, electron impact ionization, and charge exchange ionization. While photoionization is the largest contributor to the total ionization rate of interstellar helium outside 1 AU, electron impact ionization plays an increasing role close to the Sun. In the following we discuss each of the contributing processes and how the applicable rates are derived.

2.1. Photoionization rates

Since 1995, measurements of the absolute solar EUV flux with the SEM instrument on board SOHO have provided a nearly continuous data set to determine the absolute photoionization

rate of helium for the first time. SEM is one of several instruments that collectively constitute the Charge, Element and Isotope Analysis System (CELIAS) suite of instruments on SOHO. CELIAS is designed to study the composition of the solar wind (SW) and of solar and interplanetary energetic particles (Hovestadt et al. 1995). One of the specific science objectives of CELIAS is to study the composition and dynamics of interplanetary helium pickup ions, hence the inclusion of the SEM to measure the photoionization rate of the inflowing interstellar neutral helium. Using the absolute solar EUV irradiance measurements from the SEM instrument, we can determine the photoionization rate for the entire duration of the SOHO mission. The SEM helium photoionization rates are the product of the wavelength dependent EUV flux and the helium photoionization cross-section integrated over the ionization wavelength range according to:

$$\nu_0 = \int \Phi(\lambda)\sigma(\lambda)d\lambda \quad (1)$$

where ν_0 is the photoionization rate of helium in s^{-1} , Φ is the solar flux at wavelength λ in photons $cm^{-2} s^{-1}$, and σ is the photoionization cross section in cm^2 , as a function of wavelength λ . This method of integration over the product of the cross-section and the solar spectrum has been used by Banks & Kockarts (1973), Torr & Torr (1985), Torr et al. (1979), and most recently by McMullin et al. (2002b). The wavelength distribution of the integrated irradiance measured by SEM is determined by using the SOLARS22 relative solar spectrum (Woods et al. 1998). The absolute helium photoionization cross-section over the spectral region of interest is taken from Samson et al. (1994).

The uncertainty of the derived ionization rates is determined by the uncertainty of all the parameters used in the derivation. For the ionization rates deduced from the SEM observations, these are the uncertainty in the absolute solar flux and the relative uncertainty of the spectral distribution with a combined $1-\sigma$ value of 10% (McMullin et al. 2002a) and the absolute values of the cross-sections used (1% for 1σ) (Samson et al. 1994). Based on these uncertainties we have estimated the absolute uncertainty of the SEM derived helium ionization rates to $\approx 10\%$ (1σ).

2.1.1. Helium double-ionization cell measurements

This indirect determination of the photoionization rate requires parameters for the spectral distribution and cross-section data, in addition to the SEM flux measurements, to determine the ionization rate. As a check on the SEM derived ionization results they have been compared with direct measurements of the solar photoionization rate of helium by using a double-ionization helium gas cell to directly measure the photoionization rate of helium (Ogawa et al. 1997) for several specific time periods. This direct measurement of the He ionization rate is in agreement with the results obtained by using the SEM flux data.

The theory and operation of the helium double-ionization cell has been described by Samson (1966, 1967). Results from sounding rocket measurements using a similar cell have been

reported by Ogawa et al. (1997). During the SOHO mission, a helium ionization cell was flown aboard the Space Shuttle (STS-69 and STS-95) to provide direct comparison with the SEM measurements. The specific double-ionization cell used for the SEM comparison is identical to the one described by Ogawa et al. (1997). Summarizing briefly, the solar flux enters a windowless ionization cell where electron-ion pairs are produced by photons of wavelengths shortward of the ionization limit of the gas used in the cell. In this case, helium gas is cycled into the cell several times during a rocket flight, venting to the ambient atmospheric pressure between cycles. This avoids any time dependent sensitivity changes in the cell measurements due to contaminant gases, and because it is windowless, there is no time-dependent window transmission. During one operation cycle the double-ionization cell is filled with helium gas and then slowly evacuated completely several times while the ionizing flux is being measured. This cycling allows for an almost continuous purging of the cell with pure helium gas. During each pressure cycle, the ions produced per unit time are collected, and the total ion current measured is a function of the magnitude of the solar flux shortward of the ionization limit of helium. In this application, the required convolution of the solar flux and ionization cross-section is performed directly in the cell. In theory, direct measurement using ionization cells can determine the photoionization rate to an accuracy of $\pm 2\%$ (1σ), but in practice have yielded results between ± 10 and $\pm 15\%$ (1σ) (Ogawa et al. 1997).

2.1.2. Extension of the valid time period with the Mg II index

The National Oceanic and Atmospheric Administration (NOAA) Mg II index (Viereck & Puga 1999) has been found to track the variations of the solar EUV with excellent agreement (Fig. 1). This was found particularly true for the SEM EUV flux values (Viereck et al. 2001). This proxy also allows us to determine a value for the ionization rate during periods when SOHO data are not available. Therefore, the NOAA Mg II index can be used as an excellent proxy for the ionizing EUV flux. Mg II data from several NOAA satellites have been combined to form a single time series covering the period November 1978 to the present. By using the Mg II index as a proxy for the solar EUV flux, we have extended the SEM derived helium photoionization rates back to November 1978. Although EUV ionization is the most important ionization process for He, in particular at ≥ 1 AU, there are two other contributors, charge exchange with solar wind ions and electron impact ionization, that deserve additional consideration.

2.2. Charge exchange ionization

Helium charge exchange rates are generally much lower than the EUV ionization close to the Sun, adding only a small effect to the formation of the void in the neutral gas distribution and to the production of pickup He^+ . Both EUV ionization and charge exchange vary strictly as $1/r^2$ where r is the distance from the Sun; however, in the case of charge exchange, this is true once

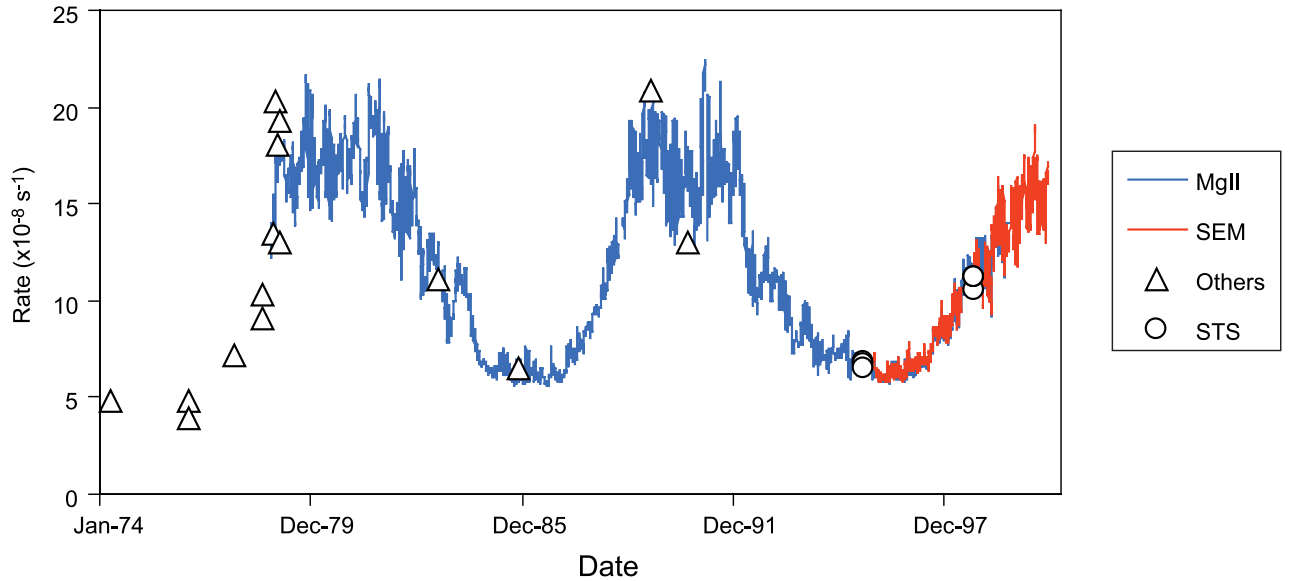
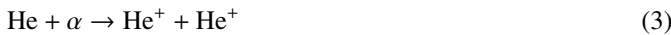


Fig. 1. The helium photoionization rate at 1 AU. The Mg II index has been fit to the SEM derived ionization rate (McMullin et al. 2002b). The Mg II and SEM derived rates are compared to occasional direct measurements from Helium Ionization cells and other methods early in the space epoch (Ogawa et al. 1997). The most recent direct measurements are from shuttle observations.

the solar wind speed is constant. For our discussions, we neglect periods when the solar wind accelerates and assume the speeds to be constant. The relevant charge exchange reactions with solar wind constituents, as discussed by Rucinski et al. (1996, 1998), are the following:



He at the left-hand side of these reactions denotes the interstellar neutral atoms, H^+ the solar wind protons, and α the solar wind α particles. At the right-hand side, H is the neutralized solar wind proton (i.e., a neutral hydrogen atom that inherited the velocity from a solar wind proton), and He^+ and He^{++} are the new-born pickup ions.

Additional sources of He^{++} due to photoionization have been determined to be insignificant. The photoionization of He^{++} from He^+ is only available from photons of energy greater than 54.4 eV (Verner et al. 1996), combined with the photoionization cross section and the scarcity of the source population of He^+ , the resultant contribution is negligible. A similar result is obtained when considering the direct photoionization of neutral He to He^{++} as is discussed in Kheifets & Bray (1998).

As can be seen, Eq. (4) describes the production of He^{++} pickup ions. In fact, it is the sole source of He^{++} pickup ions considered and hence is of extreme importance for the determination of the helium density using pickup ion observations. Gloeckler et al. (1997) have pointed out that He^{++} can be used to derive the neutral He density in the LIC without absolute calibration of the ion sensor. This is because the Ulysses Solar Wind Ion Composition Spectrometer (SWICS) instrument that is used for the observations collects both pickup ions

and the solar wind. Therefore, accuracy of the cross-section determines the error of the density determination. The accuracy of the cross-section of reaction (2) is about 40% and that of reactions (3) and (4) about 20% (Barnett et al. 1990). It should be noted that the latter rate (4) determines the accuracy of the derivation of the He density from He^{++} pickup ions Gloeckler et al. (1997).

To determine how much of an effect charge exchange has on the helium density distribution at 1 AU, the charge exchange rate is calculated, assuming a $1/r^2$ dependence, for both slow and fast solar wind conditions. In our model, we used the velocity of 450 km s^{-1} , for wind close to the solar equator (ecliptic plane) as can be derived from Ulysses observations during the first Fast Latitude Scan in 1995, and density equal to 5.5 atoms/cm^3 ; for fast solar wind we take respectively 750 km s^{-1} and 2.5 atoms/cm^3 . For the α -particle abundance in the solar wind we take 4% in the slow wind and 5% in the fast wind. The charge exchange rate is calculated according to:

$$\beta_{\text{chx},i}(v_{\text{sw}}) = n_{\text{sw}i} v_{\text{sw}} \sigma_i(v_{\text{sw}}), \quad (5)$$

where $n_{\text{sw}i}$ is the density of the appropriate solar wind population i , either of protons in the case of reaction (2) or of α particles in the case of reactions (3) and (4). The dependencies of cross-sections of these reactions on the relative velocity of colliding particles v_{sw} , adopted here as equal to the solar wind speed, were specified by Rucinski et al. (1996) following Barnett et al. (1990).

During solar minimum the solar wind is bimodal; there is an equatorial belt of the slow wind with fast streams embedded, and two areas of the fast wind at mid- and polar latitudes. Hence, one can basically expect a latitudinal dependence of the monthly-averaged charge exchange rate. During solar maximum the entire space is mostly engulfed by slow wind, with some fast wind interspersed. Therefore, one can expect

Table 1. Helium charge exchange for slow solar wind conditions.

Reaction	σ / cm^{-2}	β / s^{-1}
$\text{He} + \text{H}^+ \rightarrow \text{H} + \text{He}^+$	5.2×10^{-19}	5.0×10^{-12}
$\text{He} + \alpha \rightarrow \text{He}^+ + \text{He}^+$	2.0×10^{-17}	1.9×10^{-10}
$\text{He} + \alpha \rightarrow \text{He}^{++} + \text{He}$	2.4×10^{-16}	2.4×10^{-9}
Net charge exchange	–	2.6×10^{-9}

Table 2. Helium charge exchange for fast solar wind conditions.

Reaction	σ / cm^{-2}	β / s^{-1}
$\text{He} + \text{H}^+ \rightarrow \text{H} + \text{He}^+$	1.1×10^{-17}	1.0×10^{-10}
$\text{He} + \alpha \rightarrow \text{He}^+ + \text{He}^+$	5.4×10^{-17}	5.1×10^{-10}
$\text{He} + \alpha \rightarrow \text{He}^{++} + \text{He}$	1.9×10^{-16}	1.8×10^{-9}
Net charge exchange	–	2.4×10^{-9}

that the monthly-averaged charge exchange rate is spherically symmetric.

The expected asymmetry of the helium charge exchange rate during solar minimum is thus not large; given the large uncertainties in the cross sections and the variations of the solar wind flux, the charge exchange rate is almost spherically symmetric and relatively *invariable* over the solar cycle.

The charge exchange rates for the slow and fast wind are presented in Tables 1 and 2.

Thus charge exchange can be treated as a small additional contribution to photoionization with the same radial dependence. Contrary to photoionization, we have determined that the charge exchange rate is essentially invariable over the solar cycle. In comparison to the considerable variations in the EUV photoionization rate, the relative contribution to the total helium ionization rate varies during the solar cycle from about 3.5 to 4% during solar minimum to only 1.5% during solar maximum.

2.3. Electron impact ionization

The potential importance of ionization of the neutral interstellar helium by impact of solar wind electrons was first realized by Askew & Kunc (1984) and Rucinski & Fahr (1989, 1991), see also a compilation by Rucinski et al. (1996). They recognized through modeling that inside 1 AU the rate of electron impact ionization could be a significant fraction of the EUV ionization rate and at times may even exceed it in the immediate solar proximity (inside ≈ 0.1 AU).

Contrary to EUV ionization and charge exchange, electron impact ionization does not vary as $1/r^2$. The electron ionization rate depends strongly on the actual distribution function of the electrons in the interplanetary space, which varies greatly with solar wind conditions and distance from the Sun. Generally, it is neither Maxwellian nor even spherically symmetric (Pilipp et al. 1987a,b). For the needs of the electron impact ionization studies it is usually assumed, however, that a bi-Maxwellian distribution, consisting of a core and a halo population, is a sufficient approximation. Both of these populations are characterized by densities (n_c , n_h) and spherically symmetric

temperatures (T_c , T_h). The halo is much hotter than the core, but its density typically is at a level of $\approx 5\%$ of the core, at least up to the heliocentric distance of ≈ 4 AU (Pilipp et al. 1987a; McComas et al. 1992). Its relative contribution to the electron ionization rate increases with decreasing distance from the Sun because of different cooling rates. The increasing importance of electron impact ionization close to the Sun makes it a key player for the evaluation of the He cone close to the Sun and for pickup ion measurements inside 1 AU.

Therefore, determining the radial dependence of both distributions is of key importance for the evaluation of the electron ionization rate. Conventionally, it is assumed that both densities and temperatures vary as power laws: $T \sim T_0 r^{-a}$. The limiting cases for the temperature index a are taken as 0 and $4/3$, depending on the model for the solar wind flow. However, observations show that while the density indeed varies almost exactly as $1/r^2$, a power law is not fully adequate to describe the radial dependence of electron temperatures. Early measurements with Helios (Schwenn 1983; Marsch et al. 1989) inside 1 AU and more recent observations with Ulysses (Hoang et al. 1992; McComas et al. 1992; Phillips et al. 1995; Issautier et al. 1998, 2001) at larger heliocentric distances show that there is no single value of a that adequately describes the radial dependence of the solar wind electron temperature. Typically, the power law index for the halo population is lower than the index for the core population (Phillips et al. 1995), which means that the halo population cools slower than the core population. Currently, this conclusion is based on measurements performed outside 1 AU. The magnitude of a varies with distance from the Sun, with heliolatitude (Issautier et al. 1998) and with solar wind speed (Issautier et al. 1998; Pilipp et al. 1987a,b).

This compilation shows that there is still a large uncertainty about the distance dependence of electron ionization and its variation with solar wind conditions. However, it is evident from several studies that the radial dependence of the electron parameters are different for the slow and fast solar wind inside 1 AU. For the slow solar wind, the temperature exponent measured was 0.394 between 0.3 AU and 1 AU, and it was extrapolated to 0.68 between 0.014 AU and 0.3 AU. For the fast solar wind, the temperature exponents measured were 0.296 between 0.3 AU and 1 AU and extrapolated to 0.812 between 0.014 AU and 0.3 AU. This should lead to stronger ionization close to the ecliptic as compared with high latitudes.

Because the relative contribution of the electron ionization decreases with heliocentric distance and slow solar wind is concentrated at low latitudes during solar minimum, the total ionization rate should show a distinct latitudinal variation close to the Sun during solar minimum, which should be washed out outside 1 AU and during solar maximum. An illustration of this effect is shown in Fig. 2.

The latitudinal anisotropy of the electron ionization rate related to the persistent fast solar wind that emerges from the polar regions during solar minimum will result in an anisotropic neutral gas distribution and in a profound effect on the densities in the focusing cone. Here, the interstellar neutrals meet that have traversed all heliographic latitudes and thus have suffered losses according to the ionization rates at those latitudes. Therefore, during solar minimum the densities in the

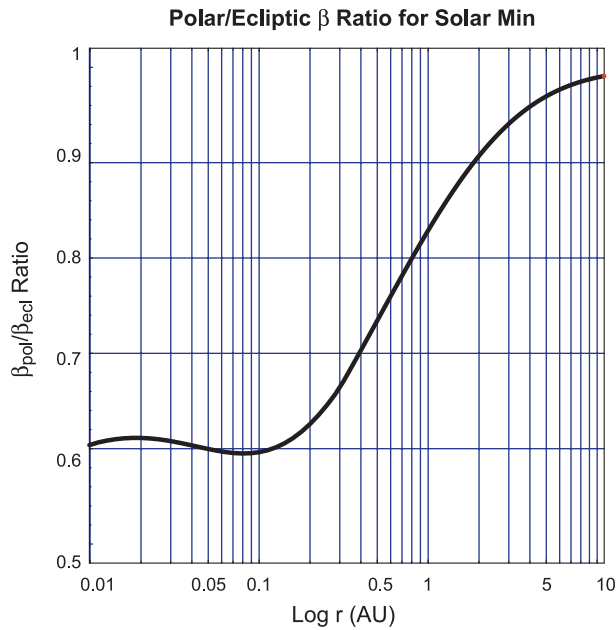


Fig. 2. Latitudinal anisotropy of the electron impact ionization rate for helium, defined as the ratio of the polar and equatorial rates, under solar minimum conditions. In lack of other data, a single Maxwellian approximation is used.

cone cannot be derived from ionization rates obtained solely in the ecliptic. These effects are most strongly apparent in observations of the cone very close to the Sun as have been performed with SOHO Ultraviolet Coronagraph Spectrometer (UVCS) (Lallement et al. 2004a). In addition, the pickup ion production rate in the cone will not be equal to the net loss rate that determines the shape of the cone and can be deduced independently from pickup ion spectra (Gloeckler et al. 2004) because the former leads to accumulation solely in the ecliptic, while the latter is composed of ionization at all latitudes. To take these effects adequately into account in the quantitative modeling of the cone structure requires a fully three dimensional treatment of the interstellar He inflow and its ionization, for which even temporal variations must be included, as will be seen below. Such a complete model is not available thus far.

For the time being the situation may be approximated by electron impact ionization rates that represent weighted averages of the relevant rates for fast and slow wind according to their relative filling factor in the inner heliosphere. Assuming that the weighting does not change significantly between 0.1 and 5 to 10 AU, it can be obtained indirectly from the heliospheric Lyman- α glow as observed with SOHO Solar Wind ANisotropies (SWAN) instrument (Bzowski 2003; Bzowski et al. 2003). From the previous solar minimum through this solar maximum the filling factor for fast wind varied from 50% at the end of 1996, to 33% at the end of 1999, to 0% at the end of 2000. This can be expressed in terms of effective ionization rates as a function of distance along the cone axis, as shown in Fig. 3, in comparison with the original standard radial dependence proposed by Rucinski & Fahr (1989), from which the ionization rates are derived. Already these rates can differ from the original rate by up to a factor of 2. This difference does not

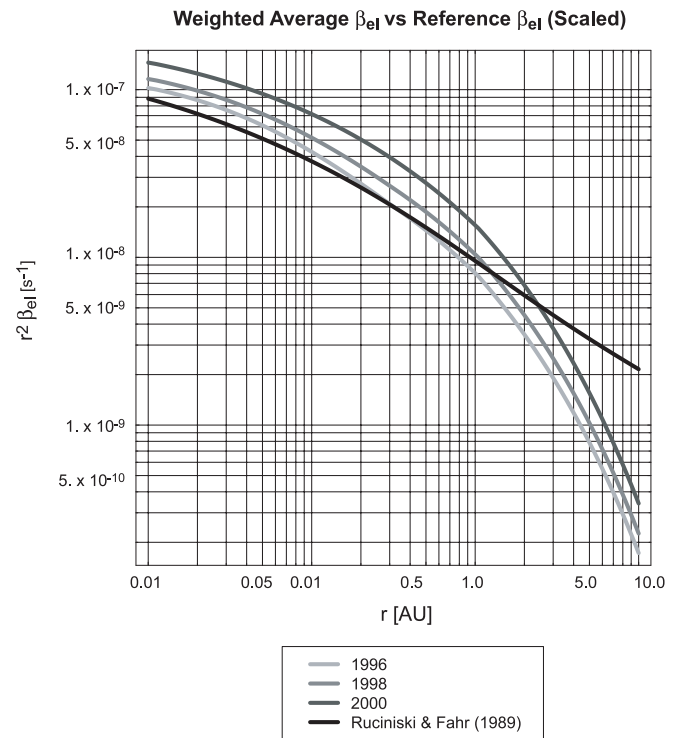


Fig. 3. Proposed weighted electron ionization rates, affecting interstellar helium in the cone, for 1996 (solar minimum), 1998 (intermediate) and 2000 (solar maximum) conditions, and the standard electron ionization rate profile proposed by Rucinski & Fahr (1989).

yet include any potential new information about the electron distribution functions and their variation.

Figure 4 shows computed hourly averages of the electron impact ionization rate close to 1 AU using electron distribution functions as observed with ACE Solar Wind Electron, Proton, and Alpha Monitor (SWEPAM) at the L1 Lagrangian point during the He cone passages in 1998, 1999, and 2000. Fluctuations by more than one order of magnitude over relatively short times are observed. Their source are variations in the electron density by up to a factor of 5 and in the temperature by a factor of 2. However, when averaged over an extended time interval of one or two months, the electron impact rate in the ecliptic plane at 1 AU shows surprisingly small variations: between the end of 1998 and the end of 2000, it stays within 1.2 and $1.6 \times 10^{-8} \text{ s}^{-1}$. It is important to note that the short-term variability observed in the electron impact ionization rates does not modulate the daily average value on longer time scales. These average values would provide a contribution to the total ionization rate of 20 to 30% of the EUV photoionization rate, but occasionally, as can be inferred from Figs. 1 and 4, the electron rate at 1 AU may reach the EUV ionization rate, which typically varies between 0.6 and $1.5 \times 10^{-7} \text{ s}^{-1}$. In essence, electron impact ionization appears to be a significant contributor to the overall ionization rate of He, with particular emphasis on the cone close to the Sun. However, the determination of these rates from electron data and modeling contains relatively large uncertainties. The cross section for electron impact ionization rate is known to about 10% (Lotz 1967). One must keep in mind, however, that any model used to

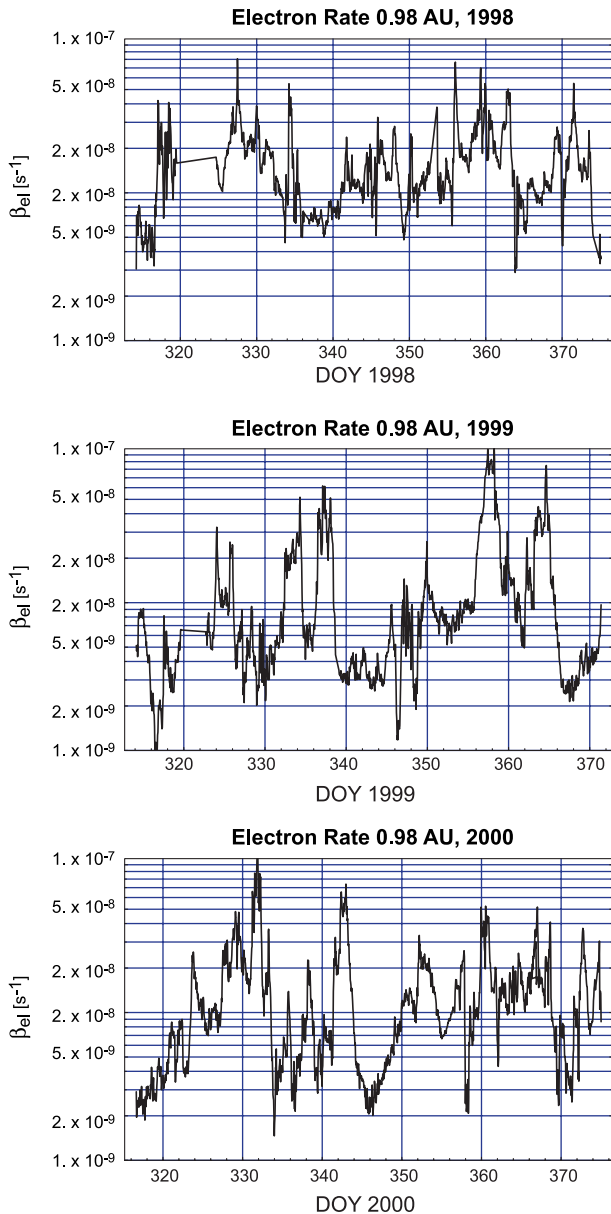


Fig. 4. Hourly electron ionization rates at 0.98 AU based on electron data measured by ACE during its passages through the helium cone in 1998, 1999, and 2000. A bi-Maxwellian was assumed for the electron density distribution.

derive the rate is based on the simplifying assumption that the electron distribution function is bi-Maxwellian. Uncertainties in the modeling of the actual shape of the electron distribution function are estimated to $\approx 25\%$. Another factor that goes into the electron ionization rate is the absolute electron density. Accurate measurements in the low energy range, most relevant here, are difficult to obtain because of the uncertainties in the electrostatic potential of the spacecraft, which leads to a low-energy cut-off in the observed electron distribution (Issautier et al. 1998, 2001). Therefore, quite frequently the electron density is deduced based on quasi-neutrality of the solar wind (the concentration of electrons is assumed equal to the concentration of solar wind protons, adding twice the concentration of solar wind α particles). Hence the uncertainty in absolute

electron density is coupled to that of solar wind density, i.e., 15 to 30%. In summary, these contributions add up to a combined uncertainty of about 50% for the absolute values.

Because all three observation methods employed in our coordinated study also return tight constraints on the total ionization rate required to explain the observations consistently, and the SOHO SEM observations provide an exact account for photoionization, it becomes possible to deduce values for electron ionization at various locations in the inner heliosphere. The neutral gas observations of atoms on indirect orbits (Witte et al. 2003) and the observations of the He cone very close to the Sun (Lallement et al. 2004c) are particularly sensitive to these ionization effects. Additionally, pickup ion observations at 1 AU require a significant ionization contribution (Gloeckler et al. 2004). From their observations, which are most sensitive close to the Sun, Witte (2004) and Lallement et al. (2004c) find values for the solar minimum that are consistent with the estimates by Rucinski & Fahr (1989), while the solar maximum value had to be increased by a factor of 3.5 (Lallement et al. 2004c). Using these values at 1 AU would lead to a relative contribution compared with EUV ionization that varies between 15 and 35%. However, Gloeckler et al. (2004) report electron ionization contributions with varying radial dependencies of 10 to 20% normalized at 1 AU. While these values can be obtained with uncertainties better than the 50% cited for the determination of the rate from the electron distributions, they still seem to disagree by about a factor of 2. However, as these observations are sensitive to different distances from the Sun, this apparent discrepancy can be understood in terms of the still unknown and quite variable radial dependence of the electron ionization rate. As a consequence, the combination of these results may in fact be used to derive the unknown radial dependence. However, in order to obtain a quantitatively accurate result, a fully 3-dimensional model of the neutral flow and ionization that also includes temporal variations has to be employed because of the observed spatial and temporal variations of the ionization. Such a model is not available at this time.

3. He 58.4 nm line profile and irradiance measurements

Observations of the interplanetary resonance glow of interstellar helium at 58.4 nm have been made by instruments aboard several spacecraft, including Prognoz 6, Voyager 1 and 2, Pioneer 10 and 11, and the Extreme Ultraviolet Explorer (EUVE). This interplanetary glow is produced by the inflowing neutral interstellar helium. Because these observations rely on resonance emissions, which are quite sensitive to the relative motion of the gas and the Sun, the knowledge of the profile of the solar 58.4 nm line is important for the interpretation of these observations. In addition, for any near-Earth spacecraft, such as EUVE, geo-corona effects can be a significant contribution to the uncertainty in the analysis of neutral helium observations. For this reason, knowledge of the absolute solar 58.4 nm irradiance, the line profile, and their temporal variability are also needed to correctly interpret the observations. In the past these parameters were usually inferred with consistency arguments.

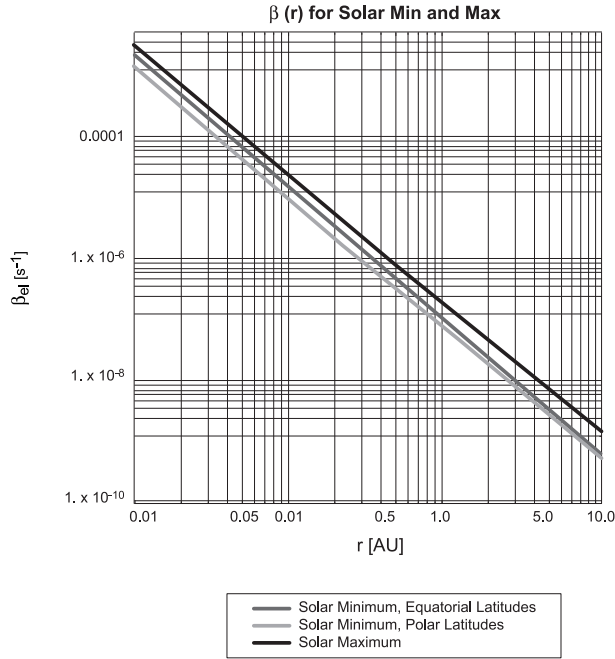


Fig. 5. Net helium ionization rates for solar minimum, equatorial latitudes; solar minimum, polar latitudes; and solar maximum, when the rate is probably spherically symmetric. The rates include ionization due to EUV, electron impact, and charge exchange.

3.1. 58.4 nm line profiles and their variations

Spectral profiles of the He I 58.4 nm line were obtained from a cadence of approximately monthly raster scan images of a quiet region near the solar disk center by the SOHO Solar Ultraviolet Measurements of Emitted Radiation (SUMER) instrument from March 1996 through February 2001. SUMER (Wilhelm et al. 1995) is a stigmatic normal incidence telescope and spectrometer, operating in the wavelength range from 46.5 to 161.0 nm, depending on the spectral order and the choice of detector. The SUMER data were corrected for the flat field, geometric distortion, and detector electronics effects, such as dead-time and local-gain depression. The Doppler width was determined by fitting a single Gaussian function and a linear background to the measured line profiles. The resulting width was corrected for the contribution of instrumental broadening. The relative uncertainty after the combined corrections is approximately 10%, with an uncertainty from the fitting procedure of 5%. As we will average over a large number of pixels (80×250), this uncertainty is negligible. For more information on the data and their reduction, see Pauluhn et al. (2001, 2002). Figure 6 shows the monthly averages of the equivalent Doppler velocities v_D calculated from the line widths of He I 58.4 nm ($v_D = c\lambda_{\text{width}}/\lambda$) as obtained by the SUMER instrument. The solid line represents an average over the entire image area of $60'' \times 250''$. In order to get an idea of the variation of the line width within one image, the upper and lower lines show the averages over the minimum 10% and maximum 10% of the line widths of the corresponding image, respectively. All values remain nearly constant over the five years of observation. The five-year average values are 36.5 km s^{-1} (with a standard deviation of 1.7 km s^{-1}) for the Doppler velocity computed from

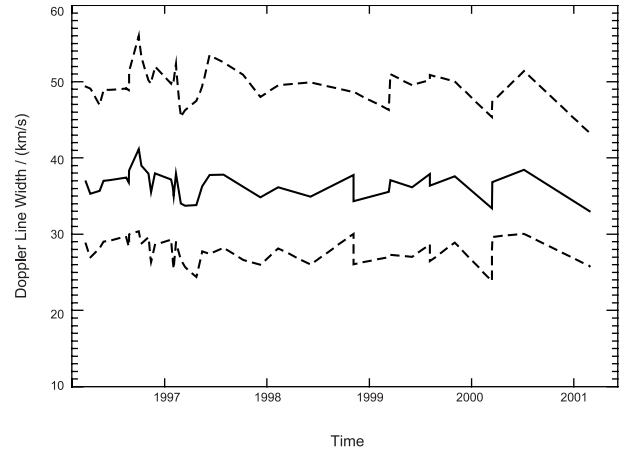


Fig. 6. Monthly averages of the Doppler velocity from the line width of He I 58.4 nm, from March 1996 to February 2001 within a quiet-Sun area of $60'' \times 250''$. The solid line shows the average over the entire image area and the upper and lower dashed lines show the averages over the minimum 10% and maximum 10% of the line widths of the corresponding image, respectively.

the full area, and 27.7 km s^{-1} and 49.5 km s^{-1} for the minimum and maximum 10% of the line widths of the considered area, respectively.

3.2. Absolute solar irradiance at 58.4 nm

The Coronal Diagnostic Spectrometer (CDS) on SOHO has been able to provide absolute 58.4 nm irradiance measurements on several occasions throughout the life of SOHO (Thompson et al. 2002). Because CDS has a small field of view, continuous monitoring of the full solar disk irradiance is not possible. Instead, special irradiance measurements, where the CDS slit is stepped over the entire solar disk, have been made on an approximately monthly basis since March 1997. More recently, this has been increased to about once every two weeks. Each observation takes more than 13 h to complete. The full spectral range of the CDS Normal Incidence Spectrometer (NIS) is observed, so that the irradiance in each emission line can be extracted by fitting the line shape. The uncertainty in the CDS absolute calibration for irradiance measurements at 58.4 nm is 18%. The uncertainty in the flat field stability over time is 10%, raising the overall uncertainty in the absolute calibration to 21% (Lang et al. 2002).

Unfortunately, the CDS 58.4 nm measurements are only available for a relatively short time period in the history of EUV measurements. As described previously, the Mg II index has been used as a proxy for Solar EUV, and may be a suitable proxy for the 58.4 nm solar irradiance as well. Since March 25, 1997, through January 29, 2001, there are 30 measurements of the full disk solar 58.4 nm irradiance from CDS. The correlation of these 30 measurements with the NOAA Mg II index is 0.98. The time period from early 1997 to 2001 is during the majority of the rise phase of solar cycle 23 and indicates that the long term variability in the 58.4 nm irradiance can be estimated using the Mg II index as a proxy.

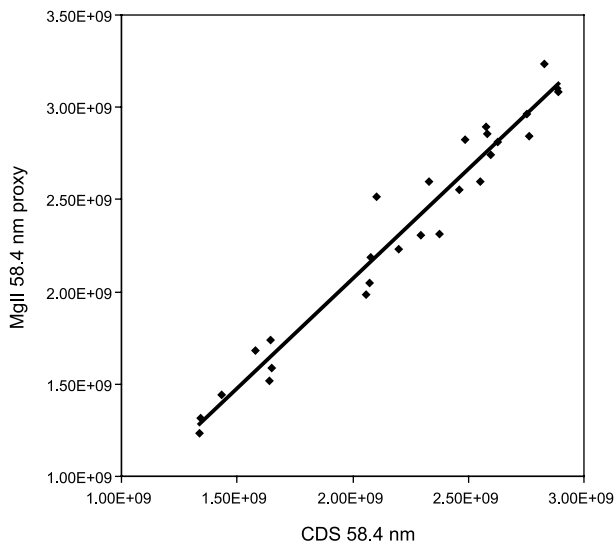


Fig. 7. Correlation of the SOHO/CDS 58.4 nm irradiance measurements with the 58.4 nm irradiance proxy fit from the Mg II index. The correlation coefficient is 0.92.

4. Conclusions

We have compiled direct observations of the parameters that affect interstellar helium inside the heliosphere. Specifically, measurements of the full disk solar EUV flux, direct measurements of ionization rates (photoionization, charge exchange, and electron impact ionization) and the line profile and intensity of the solar 58.4 nm emission have been studied. All these conditions affect the spatial distribution of neutral helium in the inner heliosphere and/or its observables, i.e., the velocity distribution of the neutrals themselves, pickup ions, and the intensity pattern of the backscattered 58.4 nm radiation. Over the past five years a comprehensive collection of this information along with the interstellar gas observations has been possible for the first time. We have critically evaluated this information in terms of its impact on the interpretation of the neutral gas, pickup ion, and UV scattering observations. During the coordinated analysis of all the contributing observations it has become possible to check our results on ionization rates and solar illumination for consistency, because each of the three different observation methods of the interstellar He distribution in the inner heliosphere, neutral gas, pickup ion, and UV backscattering measurements, provide complementary constraints on the total ionization rate of He. The interpretation of all three observations in terms of the interstellar parameters hinges upon the ionization as a loss rate for the neutrals on their way into the inner heliosphere. From the neutral gas observations on Ulysses via pickup ions at 1 AU to the UV scattering observed at the near-sun cone, these losses increase substantially, and as such, the importance of this effect on observations increases as well. Pickup ions assume a special role in this analysis: while their interpretation also requires the knowledge of the ionization as a production rate to deduce the local neutral gas density, the pickup ion velocity distribution provides a powerful diagnostic for the total ionization as a loss rate, which includes all three ionization processes (Gloeckler et al. 2004). In addition, the observation of backscattered UV in a variety of locations, ranging

from as close to the Sun as 0.15 AU to the entire sky at 1 AU accessible from the Earth's orbit, places constraints on the illuminating solar line profile.

During the coordinated observations under discussion a unique observation of the photoionization rate with 10% accuracy has been available from SOHO CELIAS SEM. Together with the knowledge that charge exchange only provides a relatively minor contribution, the combined results consistently require a substantial contribution from electron ionization (Witte 2004; Gloeckler et al. 2004; Lallement et al. 2004b; Möbius et al. 2004). As is demonstrated in this paper, the required contribution from this process appears compatible with the estimates of the electron ionization rate that are obtained from actual observations of the electrons at 1 AU. However, the absolute values of this rate can only be determined directly with an uncertainty of about 50%. In addition, we do not have any in-situ observations of the electron distribution in the crucial region inside of 1 AU, where electron ionization becomes most important. Here most of the pickup ions are produced that are observed at 1 AU (Gloeckler et al. 2004), and the He distribution observed in the cone between 0.15 and 0.5 AU with UVCS is most heavily affected by ionization very close to the Sun. Using a radial dependence for the electron ionization rate as suggested by Rucinski & Fahr (1989) to extrapolate the rate from values obtained at 1 AU to 0.15 AU or using observations of the near Sun cone to extrapolate back to 1 AU, appears to lead to results that differ by about a factor of two. As a consequence, the combined observations of the neutral He distribution close to the Sun through backscattering of the solar He I 58.4 nm line at the focusing cone and at 1 AU provide a constraint for the thus far unknown radial dependence of electron ionization. However, doing so quantitatively with better accuracy than possible now requires the use of a fully 3-dimensional model of the interstellar neutral gas flow, which includes a treatment of temporal variations. Firstly, the dependence of the rate on solar wind conditions suggests a substantial latitudinal anisotropy of this rate in the inner heliosphere. Secondly, the electron ionization rate also varies by up to one order of magnitude in time, with values occasionally reaching that of photoionization.

It should be pointed out here that all observations of the photoionization rate have been obtained in the ecliptic and are based on solar disk integrated measurements. Also, most of the electron ionization data have been obtained in the ecliptic, with the exception of the Ulysses observations, which are made outside 1.3 AU where this process becomes less and less significant. Because the latitudinal dependence plays a substantial role, as discussed above and demonstrated most notably by the Ulysses GAS observations (Witte 2004), it will be an important task for the near future to derive the actual latitudinal dependencies of the ionization rates.

Nevertheless, the continuous monitoring of the ionization rates has allowed a significant improvement of the accuracy of the results obtained from neutral gas and pickup ion observations, and improvements of the observation of electron distributions and in their modeling will allow the inclusion of this effect. In combination with the monitoring of the solar irradiance of the He I 58.4 nm line and several comprehensive

observations of its profile, even the modeling of UV backscattering measurements has been much better constrained in its parameters than has been possible in the past. Thus the use of the newly available observations of solar UV radiation and other interplanetary parameters has proven its great value in the interstellar gas analysis.

Finally, we have found proxies for the photoionization rate and for the 58.4 nm illumination that allow us to extend the validity of the analysis to interstellar He data sets obtained starting in 1978. During gaps in the solar EUV observations with the SEM instrument or for earlier time periods when no such measurements were available, the NOAA Mg II index has been identified as an excellent proxy for photoionization and for the solar illumination responsible for resonance scattering. The correlation of the SOHO/CELIAS/SEM EUV irradiance measurements to the NOAA Mg II index is 0.98, as previously discussed by Viereck et al. (2001). In this work the helium photoionization rate, as discussed by McMullin et al. (2002b), was also correlated with the Mg II index and found to have a correlation coefficient of 0.98. In addition, the correlation coefficient between the SOHO/CDS 58.4 nm irradiance observations and the Mg II index is 0.92. Because the Mg II index is available since 1978, diagnostic studies can be evaluated over a much longer period of time than is available from the direct measurement data sets. This finding will probably allow an improved reanalysis, in particular, of the UV scattering data that are available for interstellar helium since the 1970s in a search for potential long-term variations. In order to maintain the capability to perform accurate measurements of the interstellar parameters in the future and to improve its accuracy further, a continuous observation of the solar EUV and of the Mg II index with occasional absolute calibration for the He ionization rate is very important.

Acknowledgements. This work was initiated and partly carried out with support from the International Space Science Institute (ISSI) in the framework of an International Team entitled “Physical parameters of the LISM through coordinated observations of the gravitational focusing cone at 1 AU”. The authors are indebted to ISSI in Bern, Switzerland, for their support of this activity, the stimulating atmosphere, and the great hospitality, without which this coordinated analysis and its results would not have been possible. The combined effort of the participating group of scientists was supported in part under NASA SEC GI grant NAG5-10890, NASA/Caltech grant NAG 5-6912, NASA grant NAG5-5333, and Polish SCSR grant 2P03C 005 19.

References

- Askew, S. D., & Kunc, J. A. 1984, *Pl. Sp. Sci.*, 32, No. 6, 779
- Banaszkiewicz, M., Witte, M., & Rosenbauer, H. 1996, *A&AS*, 120, 587
- Banks, P. M., & Kockarts, G. 1973, *Aeronomy*, part A, Academic, San Diego, Calif.
- Barnett, C. F., Hunter, H. T., Kirkpatrick, M. I., et al. 1990, vol. ORNL-6086/V1, Oak Ridge, Tenn.
- Bzowski, M. 2003, *A&A*, 408, 1155
- Bzowski, M., Mäkinen, T., Kyrölä, E., et al. 2003, *A&A*, 408, 1165
- Chassefière, E., Bertaux, J. L., Lallement, R., & Kurt, V. G. 1986, *A&A*, 160, 229
- Daladier, F., Bertaux, J. L., Kurt, V. G., & Mironova, E. N. 1984, *A&A*, 134, 171
- Fahr, H. J., & Ripken, H. W. 1984, *A&A*, 139, 551
- Fisk, L. A., Kozlovsky, B., & Ramaty, R. 1974, *ApJ*, 190, L35
- Flynn, B., Vallergera, J., Daladier, F., & Gladstone, G. R. 1998, *J. Geophys. Res.*, 103, 6483
- Geiss, J., Gloeckler, G., Fisk, L. A., et al. 1994, *A&A*, 282, 924
- Gloeckler, G., Geiss, J., Balsiger, H., et al. 1993, *Science*, 261, 70
- Gloeckler, G., Fisk, L. A., & Geiss, J. 1997, *Nature*, 386, 374
- Gloeckler, G., Möbius, E., Geiss, J., et al. 2004, *A&A*, 426, 845
- Hoang, S., Meyer-Vernet, N., Bougeret, J.-L., et al. 1992, *Geophys. Res. Lett.*, 19(12), 1295
- Hovestadt, D., Hilchenbach, M., Bürgi, A., et al. 1995, *Sol. Phys.*, 162, 441
- Issautier, K., Meyer-Vernet, N., Moncuquet, M., & Hoang, S. 1998, *J. Geophys. Res.*, 103(A2), 1969
- Issautier, K., Skoug, R. M., Gosling, J. T., et al. 2001, *J. Geophys. Res.*, 106(A8), 15665
- Izmodenov, V., Geiss, J., Lallement, R., et al. 1999, *J. Geophys. Res.*, 104, 4731
- Kheifets, A. S., & Bray, I. 1998, *Phys. Rev. A*, 58, 4501
- Lallement, R., Raymond, J., & Vallergera, J. 2004a, *Adv. Space Res.*, 34, 46
- Lallement, R., Raymond, J., Bertaux, J.-L., et al. 2004b, *A&A*, 426, 867
- Lallement, R., Raymond, J. C., Vallergera, J., et al. 2004c, *A&A*, 426, 875
- Lang, J., Thompson, W. T., Pike, C. D., et al. 2002, *ISSI Sci. Rep. SR-002*, ed. A. Pauluhn, M. C. E. Huber, & R. von Steiger, 105
- Lotz, W. 1967, *ApJS*, 14, 207
- Marsch, E., Pilipp, W. G., Thieme, K. M., & Rosenbauer, H. 1989, *J. Geophys. Res.*, 94, No. A6, 6893
- McComas, D. J., Bame, S. J., Feldman, W. C., et al. 1992, *Geophys. Res. Lett.*, 19, No. 12, 1291
- McMullin, D. R., Judge, D. L., Hilchenbach, M., et al. 2002a, *ISSI Sci. Rep. SR-002*, ed. A. Pauluhn, M. C. E. Huber, & R. von Steiger, 135
- McMullin, D. R., Judge, D. L., Phillips, E., et al. 2002b, *Proc. of the SOHO 11 Workshop*, ESA SP-508, ed. A. Wilson, 489
- Möbius, E., Hovestadt, D., Klecker, B., et al. 1985, *Nature*, 318, 426
- Möbius, E., Klecker, B., Hovestadt, D., & Scholer, M. 1988, *Astrophys. Space Sci.*, 144, 487
- Möbius, E., Rucinski, D., Hovestadt, D., & Klecker, B. 1995, *A&A*, 304, 505
- Möbius, E., Litvinenko, Y., Grünwaldt, H., et al. 1999, *Geophys. Res. Lett.*, 26, 3181
- Möbius, E., Bzowski, M., Chalov, S., et al. 2004, *A&A*, 426, 897
- Müller, H. R., Zank, G. P., & Lipatov, A. S. 2000, *J. Geophys. Res.*, 105, 27419
- Ogawa, H. S., Phillips, E., Judge, D. L., et al. 1997, *J. Geophys. Res.*, 102, 11557
- Pauluhn, A., Rüedi, I., Solanki, S. K., et al. 2001, *Appl. Opt.*, 40, 6292
- Pauluhn, A., Lang, J., Schühle, U., et al. 2002, *ISSI Sci. Rep. SR-002*, ed. A. Pauluhn, M. C. E. Huber, & R. von Steiger, 235
- Phillips, J. L., Feldman, W. C., Gosling, J. T., & Scime, E. E. 1995, *Adv. Space Res.*, 16(9), 95
- Pilipp, W. G., Miggenrieder, H., Montgomery, M. D., et al. 1987a, *J. Geophys. Res.*, 92(A2), 1075
- Pilipp, W. G., Miggenrieder, H., Montgomery, M. D., et al. 1987b, *J. Geophys. Res.*, 92(A2), 1103
- Rucinski, D., & Fahr, H. J. 1989, *A&A*, 224, 290
- Rucinski, D., & Fahr, H. J. 1991, *Ann. Geophys.*, 9, 102

- Rucinski, D., Cummings, A. C., Gloeckler, G., et al. 1996, *Space Sci. Rev.*, 78(1), 73
- Rucinski, D., Bzowski, M., & Fahr, H. 1998, *A&A*, 334, 337
- Rucinski, D., Bzowski, M., & Fahr, H. J. 2003, *Ann. Geophys.*, 21, 1315
- Samson, J. A. R. 1966, *Adv. in Atomic and Molecular Physics*, Vol. II, ed. D. R. Bates, & I. Esterman, Academic, San Diego, Calif.
- Samson, J. A. R. 1967, *Techniques of Vacuum Ultraviolet Spectroscopy* (New York: John Wiley)
- Samson, J. A. R., He, Z. X., Yin, L., & Haddad, G. N. 1994, *J. Phys. B*, 27, 887
- Schwenn, R. 1983, *Solar Wind V*, NASA CP-2280, 489
- Thompson, W. T., McMullin, D. R., & Newmark, J. 2002, *ISSI Sci. Rep. SR-002*, ed. A. Pauluhn, M. C. E. Huber, & R. von Steiger, 211
- Torr, M. R., & Torr, D. G. 1985, *J. Geophys. Res.*, 90, 6675
- Torr, M. R., Torr, D. G., Ong, R. A., & Hinteregger, H. E. 1979, *Geophys. Res. Lett.*, 6, 771
- Verner, D. A., Ferland, G. J., Korista, K. T., & Yakovlev, D. G. 1996, *ApJ*, 465, 487
- Viereck, R. A., & Puga, L. C. 1999, *J. Geophys. Res.*, 104, 9995
- Viereck, R. A., Puga, L. C., McMullin, D. R., et al. 2001, *Geophys. Res. Lett.*, 28, 1343
- Weller, C. S., & Meier, R. R. 1981, *ApJ*, 246, 386
- Wilhelm, K., Curdt, W., Marsch, E., et al. 1995, *Sol. Phys.*, 162, 189
- Witte, M., Rosenbauer, H., Keppler, E., et al. 1992, *A&AS*, 92, 333
- Witte, M., Rosenbauer, H., Banaszkiwicz, M., & Fahr, H. 1993, *Adv. Space Res.*, 13, 121
- Witte, M., Banaszkiwicz, M., & Rosenbauer, H. 1996, *Space Sci. Rev.*, 78, 289
- Witte, M., Banaszkiwicz, M., Rosenbauer, M., & McMullin, D. R. 2003, *Adv. Space Res.*, in press
- Witte, M. 2004, *A&A*, 426, 835
- Woods, T., Ogawa, H. S., Tobiska, K., & Farnil, F. 1998, *Sol. Phys.*, 177, 511